

Self-triggered coordination of distributed renewable generators for frequency restoration in islanded microgrids: A low communication and computation strategy

Yulin Chen^a, Donglian Qi^{a,b,*}, Hongxun Hui^{c,*}, Shaohua Yang^c, Yurun Gu^d, Yunfeng Yan^b, Yi Zheng^b, Jiangfeng Zhang^e

^a Hainan Institute of Zhejiang University, Yazhou Bay Science and Technology City, Sanya, 572025, Hainan Province, China

^b Zhejiang University, 38 Zheda Road, Hangzhou, 310027, Zhejiang Province, China

^c University of Macau, Avenida da Universidade, Taipa, 999078, Macao, China

^d Macau University of Science and Technology, Avenida Wai Long, Taipa, 999078, Macao, China

^e State Grid Zhejiang Electric Power Research Institute, Zhaohui 8th District, Gongshu District, Hangzhou, 310027, Zhejiang Province, China

ARTICLE INFO

Keywords:

Distributed renewable generators
Frequency restoration
Distributed control
Self-triggered mechanism
Control efficiency
Islanded microgrid

ABSTRACT

Microgrid provides a promising solution to consume more distributed renewable energies. To coordinate the increasingly developed distributed renewable generators in a high flexibility and high efficiency way, distributed event-triggered mechanisms have been widely investigated in the literature to reduce the communication requirement and hence improve the control performance of microgrids. However, most of the event-triggered mechanisms mandate continuous calculation of complicated triggering conditions, which may in turn impose the computation burden of the controller and increase additional energy cost. To this end, this paper presents a distributed self-triggered control strategy for the frequency restoration in islanded microgrids with the aid of a linear clock. With this self-triggered solution, each distributed generator's controller decides its own control and communication actions based on monitoring the linear clock, which excludes continuous calculation of any triggering conditions. Thus, the communication and computation costs can be reduced simultaneously. Moreover, Zeno behavior can be naturally excluded by the above design. The results of theoretical analysis and simulations show that the proposed distributed self-triggered control scheme can effectively coordinate distributed renewable generators with very low communication and computation requirements. Therefore, this research can improve the coordination efficiency of microgrids greatly, which is very useful for guiding the efficient operation of large-scale distributed renewable generators.

1. Introduction

To mitigate climate change, sustainable and low-carbon use of energy has become the focus of human attention [1]. Two major challenges for decarbonization of energy systems include renewable transition planning and sustainable systems operations [2]. From the perspective of renewable transition planning, the decarbonization promotes the development of distributed generators (DGs) around the world, such as photovoltaic and wind generators. From the view of sustainable systems operations, microgrids (MGs) with flexible operation ability are increasing rapidly to integrate and coordinate local loads and DGs [3], so that the investment into long-distance electricity transmission can be decreased [4]. However, compared with traditional large-scale power systems, the stable operation of MGs is more challenging [5]. The first reason is that the power output of DGs in MGs is easily impacted by

changeable weather conditions, which bring more fluctuations to MGs. The second reason is that the regulation resources in MGs are generally less than the traditional generating units in large-scale power systems [6].

To maintain the stability of MGs, two control processes have been proposed and widely used in the real-time operation, i.e., the primary control and the secondary control of DGs [7]. The primary control handles quickly stabilizing the frequency and voltage of MGs when disturbances occur, which is prevalently achieved by droop control [8]. The secondary control is to compensate for the frequency and voltage deviations caused by primary droop control or during fault conditions. It can be achieved by centralized, decentralized and distributed methods, among which the distributed secondary control with local decision making and neighboring communication has the advantages of both scalability and reliability [9]. Since DGs are usually located dispersedly, the

* Corresponding authors.

E-mail addresses: qidl@zju.edu.cn (D. Qi), hongxunhui@um.edu.mo (H. Hui).

<https://doi.org/10.1016/j.adapen.2023.100128>

Received 20 December 2022; Received in revised form 17 February 2023; Accepted 18 February 2023

Available online 23 February 2023

2666-7924/© 2023 The Authors. Published by Elsevier Ltd. This is an open access article under the CC BY-NC-ND license (<http://creativecommons.org/licenses/by-nc-nd/4.0/>)

Nomenclature

ω_i	The angular frequency of DG i , Hz
ω_i^*	The set point of the primary control of DG i , Hz
ω_i^{\max}	The maximum angular frequency of DG i , Hz
ω_i^{\min}	The minimum angular frequency of DG i , Hz
ω_i^r	The reference angular frequency of DG i , Hz
P_i	The active power output of DG i , kW
P_i^{\max}	The minimum active power output of DG i , kW
u_i^ω	The frequency restoration control input of DG i
u_i^P	The active power sharing control input of DG i
k_ω	The coupling gain of frequency restoration control
k_P	The coupling gain of active power sharing control
ε	The sensitivity parameter of frequency restoration control
$t_k^{\omega i}$	The k th triggering time instant of DG i
θ_i^ω	The linear clock of frequency restoration of DG i
θ_i^P	The linear clock of active power sharing of DG i
δ_i	The sensitivity parameter of active power sharing control

distributed secondary control is more applicable to MGs with massive DGs than the other two ways.

To provide more operation flexibility of DGs, in recent years, there have emerged a lot of excellent papers working on distributed secondary control [10]. For example, Xin et al. [11] first use multi-agent system-based distributed control method to achieve active power sharing in MGs in a fully distributed way. Bidram et al. [12] propose the first distributed frequency/voltage restoration control strategy with a leader-follower consensus algorithm. Then, they detailedly discuss how to achieve distributed secondary control in small-scale power systems using multiagent cooperative control theory [13]. Zhang et al. [14] use distributed estimation algorithm to achieve distributed secondary control in microgrid. Hui et al. [15] propose a distributed control for frequency restoration considering both distributed generators and load resources in urban MGs. These distributed secondary control schemes mentioned above are all based on continuous control and communication assumption, i.e., the control actions and communications are successive with a small fixed sampling period. However, this assumption would degrade the efficiency of the control system. On the one hand, the continuous control is usually implemented by discretization. In order to guarantee the system stability in the worst cases, the fixed sampling time is always selected consecutively, generating a very frequent communication and computation. It is too much for the DGs with microprocessors that are usually running with limited computing and communication capability. On the other hand, with the continuous control and communication assumption, the controller will take control and communication actions even at steady states, leading to a wasteful use of the communication and computation resources and hence causing additional energy waste. Therefore, improving the efficiency of the distributed secondary control system can not only reduce system burden, but also reduce energy consumption of control and communication, which can highly improve the flexibility and efficiency of MGs, and also contributes to decarbonization, especially for the system with large-scale DGs [16].

To reduce the cost of limited resources, more attention is paid to distributed event-triggered secondary control strategies. With the event-triggered mechanism, each DG determines the triggers of its controller by continuously calculating and monitoring a complex triggering condition, leading to aperiodic and intermittent neighboring communication rather than continuous neighboring communication. A trigger means one time control action and one time communication with neighbors. Hence, the communication burden can be greatly reduced in this way. The related work includes: Fan et al. [17] design a distributed event-triggered consensus-like nonlinear state feedback con-

trol to solve the problem of reactive power sharing, with which the communication requirement is greatly reduced. Chen et al. [18] design a distributed event-triggered mechanism for frequency restoration control in MGs. With the aid of a distributed estimator, Chen et al. [19] design a distributed frequency restoration controller with event-triggered communications. After that, the authors in [20] solve both restoration and power sharing secondary control problems simultaneously with different event-triggered mechanisms [21]. By decoupling the frequency restoration and active power allocation objectives and using the event-triggered consensus algorithm in [22] to the active power sharing control, Wang et al. [23] achieve both secondary control objectives with high communication efficiency. Then, Abdolmalek et al. [24] develop a distributed event-triggered secondary controller that can naturally exclude Zeno behavior, which simplifies the controller design a lot. To tolerate communication time delay, a novel event-triggered control protocol is proposed by Xie and Lin [25] for the voltage restoration in AC MGs. To achieve faster convergence, a finite-time distributed event-triggered secondary frequency and voltage control for islanded AC MGs is proposed by Choi et al. [26]. After that, Qian et al. [27] propose a dynamic event-triggered controller for the secondary control in DC MGs, with which the inter-event time between triggers can be enlarged and hence the communications can be further reduced. However, all the distributed event-triggered control schemes mentioned above mandate continuous calculation of a triggering condition, which would in turn increase the computation cost of the controller [28]. It implies the fact that the event-triggered mechanism has to sacrifice the computation efficiency in exchange for the communication efficiency.

To overcome this dilemma, one needs to try to reduce the computation cost while maintaining communication reduction. To this end, Chen et al. [29] estimate the upper bound of the time intervals between the triggers of controllers, and use this upper bound to enlarge the triggering condition checking period to reduce the computation burden. But, the computation cost would not be much reduced if the triggering condition is very complex. In fact, the computation requirement can be further reduced by developing a distributed self-triggered mechanism [30]. By self-triggered control, it means that each controller determines its triggers using the information at previous time instant without involving the calculation of any triggering condition [31]. To the best of the authors' knowledge, rare study can coordinate distributed generators with high communication efficiency and computation efficiency simultaneously, which motivates our research in this paper.

In this paper, a distributed self-triggered control strategy for the coordination of DGs is proposed to solve the problem of frequency restoration in islanded MGs. The contributions of this paper lie in:

- 1) For frequency restoration control, a linear clock is introduced to help design the self-triggered controller, with which any calculation of triggering condition is not required. Therefore, the communication and computation can be reduced simultaneously.
- 2) By introducing the signum function and linear clock, Zeno behavior of the designed controller can be naturally excluded due to the select parameter ε , which also determines the trade-off between the control performance and the number of triggering times.
- 3) By using the similar designing principle, the active power sharing control is also achieved with the self-triggered mechanism, thus both objectives of frequency restoration and active power sharing are realized with high efficiency.

With the proposed strategy, the coordination efficiency of distributed renewable generators in microgrids is greatly improved, which is very useful for guiding the efficient operation of large-scale distributed renewable generators.

The rest of this paper is organized as follows: Traditional distributed secondary control in islanded MGs is introduced in Section 2. In Section 3, our main results of the distributed self-triggered mechanisms designing for the frequency restoration and active power sharing of MGs are provided. In Section 4, the effectiveness of the proposed controller

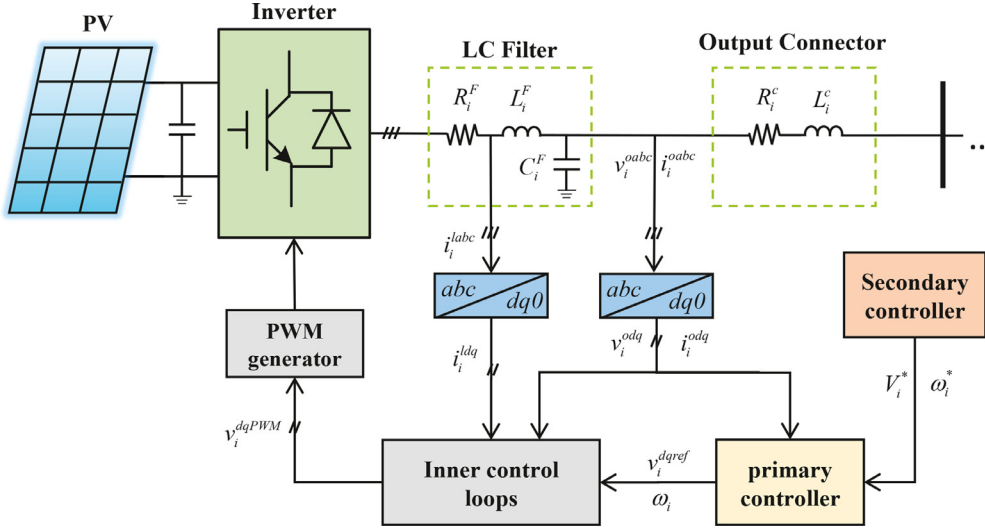


Fig. 1. Block diagram of an inverter-based DG.

is validated by several simulation results. Finally, Section 5 concludes our work in this paper.

2. Traditional distributed secondary control in islanded microgrids

In this paper, DGs are considered as photovoltaic (PV) systems, which can be modeled as inverter-based voltage sources with photovoltaic panes [32]. The block diagram of a DG is illustrated in Fig. 1. In this constructure, the PV system is connected to the MG through a DC/AC inverter, an LC filter and an output line, which is also termed as output connector. For the control of the inverter-based DG, it contains the inner voltage loop, inner current loop, and PWM controller in a cascade configuration. The time scale of these control loops is very short, and hence can be neglected safely when we focus on the secondary control level. One can refer to [13] for the detailed dynamics of these inner control loops.

For the primary control in islanded MGs, it provides reference signals to the inner control loops. Droop control is one of the widely used strategies to stabilize the frequency and voltage in a trivial amount of time. Droop mechanism emulates the $P - \omega$ and $V - Q$ relationships of the conventional synchronous generators [33]. For $P - \omega$ droop mechanism, it can be represented by

$$\omega_i = \omega_i^* - m_i P_i \quad (1)$$

where m_i satisfies [34]

$$m_i = \frac{\omega_i^{\max} - \omega_i^{\min}}{P_i^{\max}}, \quad (2)$$

On this basis, the droop-based primary control makes DGs share their active power according to their droop coefficients. Specifically,

$$m_1 P_1 = m_2 P_2 = \dots = m_N P_N. \quad (3)$$

It is worth noting that the maximum power in the Eq. (2) is the dynamic maximum available power, while not the rated installed capacities. That is to say, the droop coefficient is based on the real-time available power output of each DG, which is dynamic with time.

In this paper, for the secondary control in islanded MGs, the main control objective is to restore the operating frequency in an islanded MG back to the reference value based on distributed cooperative control. That is, achieving the following objective in a distributed manner,

$$\lim_{t \rightarrow \infty} \omega_i(t) = \omega_i^r. \quad (4)$$

For distributed secondary control, since the control algorithm is placed at DGs' local, in order to achieve the global objective, the communication network plays a vital role. Mathematically, the communication network can be represented by an undirected graph $\mathcal{G} = (\mathcal{V}, \mathcal{E}, \mathcal{A})$. \mathcal{V} denotes the vertex set, representing the set of DGs in MGs. \mathcal{E} denotes the edge set, representing the set of communication links between DGs. $\mathcal{A} = [a_{ij}]_{n \times n}$ is the adjacency matrix, characterizing the communication relationship between DGs, where n is the total number of DGs. $a_{ij} = 1$ indicates DG i can receive information from DG j . Thus, DG j is called the in-neighbor of DG i . If $a_{ij} = 0$, it means there exists no communication between DG i and DG j . A path between two DGs (e.g., DG i and DG j) is defined as a vertex sequence $s_1, s_2, \dots, s_l, \dots, s_k$, where $s_1 = i$, $s_k = j$, and $s_j \in \mathcal{E}$. A communication network is called connected if there exists a path between every two DGs. The neighbor set of DG i is denoted by \mathcal{N}_i . The number of DG i ' neighbors, representing by d_i , is called the degree of DG i . Then, the Laplacian matrix is defined by $L = D' - \mathcal{A}$, where $D' = \text{diag}\{d_1, d_2, \dots, d_n\}$.

To realize the global control objective, the following assumption is made throughout this paper.

Assumption 1: The communication network is undirected and connected.

In general, by turning the set point ω_i^* of the primary control in (1) via the following auxiliary control inputs u_i^ω , the objective of (4) can be achieved in a distributed manner [12,35,36],

$$u_i^\omega = -k_\omega \left[\sum_{j \in \mathcal{N}_i} a_{ij} (\omega_i - \omega_j) + b_i (\omega_i - \omega^r) \right], \quad (5)$$

in which $\dot{\omega}_i = u_i^\omega$; $k_\omega > 0$; $b_i \in \{0, 1\}$ is the pinning gain, indicating the access to the reference angular frequency.

Note that the distributed control law (5) only involves the local state, the neighbors' information, and the reference angular frequency (if $b_i = 1$), it means that the distributed controller can be deployed at DGs' local, and the communication is localized as well. Therefore, the distributed frequency restoration controller has better reliability and scalability compared to the traditional centralized one, and hence is more adapted to coordinate the distributed energy resources in MGs.

However, the frequency restoration control itself may lead to bad active power allocation compared to the droop-based primary control. The reason is that there are two degrees of freedom in the secondary control of MGs, it means the two control objectives, i.e., the frequency restoration control and the active power sharing control, are deeply coupled, as expressed in (1). If we only control one of them, the other would be affected. Therefore, it is expected to maintain the same power sharing

pattern as the droop control after the frequency restoration controller being applied.

To meet this requirement, one needs to coordinate the outputs of DGs. This problem is usually transformed into a consensus problem with the following auxiliary control input

$$u_i^P = -k_p \sum_{j \in \mathcal{N}_i} a_{ij}(m_i P_i - m_j P_j), \quad (6)$$

where $m_i \dot{P}_i = u_i^P$; $k_p > 0$.

Therefore, the set point of the primary control can be given by

$$\omega_i^* = \int (u_i^{\omega} + u_i^P) dt, \quad (7)$$

with which the frequency restoration objective can be achieved, and at the same time, the active power can be shared properly according to DGs' droop coefficients.

However, it should be noted that the controller (5) and the controller (6) are based on the assumption of continuous controller updates and communications. This would result in a wasteful use of the local resources of DGs, which may degrade the effectiveness and performance of MGs.

Self-triggered control can solve this problem by triggering the distributed controller only when necessary. The triggers are determined when the stability condition is about to be violated. Accordingly, the self-triggered control may not tolerate too much longer time delay. Therefore, the following assumption should be held.

Assumption 2: It is assumed that the communication delay among DGs is much smaller compared with the communication interval in between triggers.

3. Distributed self-triggered secondary controller design

In this section, we first design a distributed self-triggered controller for the frequency restoration in islanded MGs based on a linear clock, which can exclude Zeno behavior naturally and does not involve continuously computing any triggering condition. Meanwhile, we provide the theoretical analysis of the proposed controller in detail. In addition, based on the same design principle, we design a similar distributed self-triggered control scheme for the active power sharing in islanded MGs as well.

3.1. Self-triggered frequency restoration controller design

Preliminary, the frequency consensus error is denoted by

$$D_i = \sum_{j \in \mathcal{N}_i} a_{ij}(\omega_i - \omega_j) + b_i(\omega_i - \omega^r), \quad (8)$$

Then, we define the following function

$$\text{sign}_{\varepsilon}(x) = \begin{cases} \text{sign}(x) & \text{if } |x| \geq \varepsilon \\ 0 & \text{otherwise,} \end{cases} \quad (9)$$

where $\varepsilon \geq 0$ is the sensitivity parameter indicating the convergence accuracy.

By using the defined function and the consensus error, the frequency restoration control input with a linear clock is defined as

$$\begin{cases} u_i^{\omega}(t) = -\text{sign}_{\varepsilon}(\hat{D}_i(t)) \\ \dot{\theta}_i^{\omega}(t) = -1, \end{cases} \quad (10)$$

where

$$\hat{D}_i(t) = D_i(t_k^{\omega i}) \text{ for } t \in [t_k^{\omega i}, t_{k+1}^{\omega i}), \quad (11)$$

in which $t_k^{\omega i}$ is determined by

$$t_k^{\omega i} = \inf\{t > t_{k-1}^{\omega i} | \theta_i^{\omega}(t) = 0\}. \quad (12)$$

Let $\theta_i^{\omega}(t)$ satisfy the evolution of

$$\theta_i^{\omega}(t^+) = \begin{cases} \max\left\{\frac{|D_i(t)|}{4(|\mathcal{N}_i| + b_i)}, \frac{\varepsilon}{4(|\mathcal{N}_i| + b_i)}\right\} & \text{if } \theta_i^{\omega}(t) = 0 \\ \theta_i(t) & \text{otherwise,} \end{cases} \quad (13)$$

where $|\mathcal{N}_i|$ is the cardinal number of \mathcal{N}_i , indicating the number of DG i 's neighbor.

The principle behind this controller design is: the controller only updates its state $D_i(t)$ by using the local state and the neighboring states at the triggering time instant $t_k^{\omega i}$ [cf. (10) and (11)]; otherwise, u_i^{ω} remains unchanged during the time intervals between triggers. The triggering time instants are determined by the linear clock of $\theta_i^{\omega}(t)$, which decays linearly according to t with the dynamic of $\dot{\theta}_i^{\omega}(t) = -1$. When the clock $\theta_i^{\omega}(t)$ decays to 0, the time t is defined as a triggering time instant, and at the same time, the clock $\theta_i^{\omega}(t_k^{\omega i})$ is updated by $\max\left\{\frac{|D_i(t_k^{\omega i})|}{4(|\mathcal{N}_i| + b_i)}, \frac{\varepsilon}{4(|\mathcal{N}_i| + b_i)}\right\}$.

Therefore, the controller only needs to monitor the clock θ_i^{ω} to determine the triggering time instants without involving computation for any triggering condition. This feature makes the controller reduce the computation burden significantly compared to the event-triggered controllers.

Then, we can conclude that the triggering times naturally define the evolution of θ_i^{ω} , namely:

$$t_{k+1}^{\omega i} = t_k^{\omega i} + \begin{cases} \frac{|D_i(t_k^{\omega i})|}{4(|\mathcal{N}_i| + b_i)} & \text{if } |D_i(t_k^{\omega i})| \geq \varepsilon \\ \frac{\varepsilon}{4(|\mathcal{N}_i| + b_i)} & \text{if } |D_i(t_k^{\omega i})| < \varepsilon. \end{cases} \quad (14)$$

Thus, we immediately argue that, for each DG i , the time interval between every two adjacent triggering time instants has a lower bound, i.e., for any $k \geq 1$,

$$t_{k+1}^{\omega i} - t_k^{\omega i} \geq \frac{\varepsilon}{4 \max\{|\mathcal{N}_i| + b_i\}}. \quad (15)$$

This means the self-triggered controller can naturally exclude Zeno behavior.

For the concept of Zeno behavior in continuous control, Zeno behavior means an infinite number of triggers in a finite time period, occurs [37]. However, in practice, the continuous control is usually realized by discretization. Thus, Zeno behavior for the discretized continuous control means successive redundant triggers occur over a finite period. In other words, it means the controller trigger happens at every sampling time during a finite period, which indicates a failure of self-triggered mechanism design. Therefore, it is important to prove the exclusion of Zeno behavior when one designs an event-triggered or a self-triggered controller.

For most of the existing researches regarding event-triggered or self-triggered controllers, the exclusion of Zeno behavior is usually proved by deriving a positive lower bound of the time interval between every two adjacent triggering time instants. However, rather complicated calculations are involved when acquiring the lower bound. Whereas, our self-triggered controller can naturally exclude Zeno behavior due to the definition of the linear clock, showing the superiority of the proposed self-triggered controller.

The following Theorem states the convergence correctness of the proposed distributed self-triggered frequency restoration controller.

Theorem 1: For an MG with N DGs under **Assumption 1** and **Assumption 2**, in which one DG has access to the reference frequency, if each DG is equipped with the designed controller (10), triggering at the time instants of (12) that is monitored by the linear clock $\theta_i^{\omega}(t)$ evolved according to (13), then the frequency restoration objective of (4) can be achieved with a desired convergence error ε .

Proof: We first define the tracking error by

$$e_i(t) = \omega_i(t) - \omega^r, \quad (16)$$

Then, we have $D(t) = He(t)$, in which $H = L + B$, $B = \text{diag}\{b_1, b_2, \dots, b_N\}$, $D = [D_1, D_2, \dots, D_N]^T$ and $e = [e_1, e_2, \dots, e_N]^T$.

Considering the following candidate Lyapunov function

$$V(e(t)) = \frac{1}{2} e^T H e \geq 0, \quad (17)$$

we can derive the derivative of $V(t)$ as

$$\dot{V} = e^T H \dot{e} = - \sum_{i=1}^N D_i \text{sign}_\varepsilon(\hat{D}_i) = - \sum_{i: |\hat{D}_i| \geq \varepsilon} D_i \text{sign}_\varepsilon(\hat{D}_i). \quad (18)$$

According to (10) and (14), we observe that, for $t \in [t_k^{\omega_i}, t_{k+1}^{\omega_i})$, $\hat{D}_i = D_i(t_k^{\omega_i}) \leq -\varepsilon$ indicates $\dot{\omega}_i = 1$ [cf. (10)]. It means that ω_i increases, and hence \hat{D}_i increases with the quantity of $(|\mathcal{N}_i| + b_i)(t - t_k^{\omega_i})$ in between $t_k^{\omega_i}$ and t . And ω_j for all $j \in \mathcal{N}_i$ may decrease with the quantity of $(t - t_k^{\omega_i})$, hence \hat{D}_i may increase with the quantity of $|\mathcal{N}_i|(t - t_k^{\omega_i})$ in between $t_k^{\omega_i}$ and t either. So, we have

$$D_i(t) < \hat{D}_i + 2(|\mathcal{N}_i| + b_i)(t - t_k^{\omega_i}) \leq \frac{\hat{D}_i}{2}, \quad (19)$$

in which we have used the relation $t - t_k^{\omega_i} \leq \frac{-\hat{D}_i}{4(|\mathcal{N}_i| + b_i)}$.

Similarly, for $t \in [t_k^{\omega_i}, t_{k+1}^{\omega_i})$ and $\hat{D}_i \geq \varepsilon$, we can derive

$$D_i(t) > \frac{\hat{D}_i}{2}. \quad (20)$$

Inequalities (19) and (20) mean D_i and \hat{D}_i have the same sign when $|\hat{D}_i| \geq \varepsilon$. So we have $D_i \text{sign}_\varepsilon(\hat{D}_i) = |D_i|$ for $|\hat{D}_i| \geq \varepsilon$.

Moreover, from (19) we can derive that, for $\hat{D}_i \leq -\varepsilon$,

$$|D_i(t)| = -D_i(t) > -\hat{D}_i - 2(|\mathcal{N}_i| + b_i)(t - t_k^{\omega_i}) \geq \frac{|\hat{D}_i|}{2}. \quad (21)$$

Combining it with (20), we have $|D_i(t)| > \frac{|\hat{D}_i|}{2}$. Therefore, we can deduce from (18) that

$$\dot{V} = - \sum_{i: |\hat{D}_i| \geq \varepsilon} D_i \text{sign}_\varepsilon(\hat{D}_i) < - \sum_{i: |\hat{D}_i| \geq \varepsilon} \frac{|\hat{D}_i|}{2} \leq - \sum_{i: |\hat{D}_i| \geq \varepsilon} \frac{\varepsilon}{2}. \quad (22)$$

Inequality (22) implies that when $|\hat{D}_i| < \varepsilon$ for all $i \in \{1, 2, \dots, N\}$, $\dot{V}(t) = 0$. In this sense, the system reaches stability. Thus, we can conclude that, with the proposed distributed self-triggered frequency restoration controller, the control objective (4) can be achieved with a convergence error of $|\sum_{j \in \mathcal{N}_i} a_{ij}(\omega_i - \omega_j) + b_i(\omega_i - \omega^*)| < \varepsilon$. ■

Note that the proposed self-triggered controller is not asymptotically convergent, but converges with a desired error. Nevertheless, it is applicable for the secondary control of MGs as long as ε is chosen to be small enough. In addition, it can be seen from (10), (13), and the convergence error $|\sum_{j \in \mathcal{N}_i} a_{ij}(\omega_i - \omega_j) + b_i(\omega_i - \omega^*)| < \varepsilon$ that, the choice of ε prescribes the trade-off between the number of triggers and the accuracy of convergence. Specifically, a smaller ε means a smaller convergence error, but more triggers. Indeed, small control error is important to the system operation, while over-triggering is certainly a drawback from the perspective of an efficient use of limited communication and computation resources. If one chooses $\varepsilon = 0$, the controller will degrade to a traditional distributed secondary controller with no convergence error.

It should also be pointed out that, different from the existing event-triggered distributed secondary controllers, the designed linear clock $\theta_i(t)$ and the employment of $\text{sign}_\varepsilon(\cdot)$ result in a linear evolution of the proposed controller. Furthermore, as (13) illustrate, the triggers during the transient period are aperiodic and intermittent, rather than continuous. Since no triggering condition computation is involved, the communication and computation costs can be greatly reduced.

3.2. Self-triggered power sharing controller design

In order to maintain the same power sharing pattern as what droop mechanism does while reducing the communication and computation

requirements, a distributed self-triggered power sharing controller is proposed based on a similar principle in this subsection.

Similarly, we first denote a consensus error for the active power

$$A_i = \sum_{j \in \mathcal{N}_i} a_{ij}(p_i - p_j), \quad (23)$$

in which we let p_i represent $m_i P_i$.

Then, we design the control input with a linear clock by

$$\begin{cases} u_i^P(t) = -\text{sign}_\delta(\hat{A}_i(t)) \\ \dot{\theta}_i^P(t) = -1. \end{cases} \quad (24)$$

in which $\hat{A}_i(t) = A_i(t_k^{P_i})$ for $t \in [t_k^{P_i}, t_{k+1}^{P_i})$, where $t_k^{P_i}$ is the k th ($k = 1, 2, \dots$) triggering time instant of DG i , which can be similarly defined by

$$t_k^{P_i} = \inf\{t > t_{k-1}^{P_i} | \theta_i^P(t) = 0\}. \quad (25)$$

Analogously, the evolution of $\theta_i^P(t)$ is designed as

$$\theta_i^P(t^+) = \begin{cases} \max\left\{\frac{|A_i(t)|}{4|\mathcal{N}_i|}, \frac{\delta}{4|\mathcal{N}_i|}\right\} & \text{if } \theta_i^P(t) = 0 \\ \theta_i(t) & \text{otherwise.} \end{cases} \quad (26)$$

Thus, we also have

$$t_{k+1}^{P_i} = t_k^{P_i} + \begin{cases} \frac{|A_i(t_k^{P_i})|}{4|\mathcal{N}_i|} & \text{if } |A_i(t_k^{P_i})| \geq \delta \\ \frac{\delta}{4|\mathcal{N}_i|} & \text{if } |A_i(t_k^{P_i})| < \delta, \end{cases} \quad (27)$$

that is $t_{k+1}^{P_i} - t_k^{P_i} \geq \frac{1}{4 \max(|\mathcal{N}_i|)}$ for all $i \in \{1, 2, \dots, N\}$ and all $k \in \{0, 1, 2, \dots\}$, and hence Zeno behavior is naturally excluded as well.

By this design, we have the following theorem.

Theorem 2: For an MG with N DGs under Assumptions 1 and 2, if each DG is equipped with the controller (24), triggering at the time instants of (25) monitored by the linear clock $\theta_i^P(t)$ that evolves according to (26), then the active power sharing objective can be achieved with a desired convergence error δ .

Proof: For the power sharing controller, we consider the following candidate Lyapunov function

$$V(p(t)) = \frac{1}{2} p^T L p \geq 0, \quad (28)$$

with $p = [p_1, p_2, \dots, p_N]^T$.

Thus, the derivative of (28) is

$$\dot{V} = p^T L \dot{p} = - \sum_{i=1}^N A_i \text{sign}_\delta(\hat{A}_i) = - \sum_{i: |\hat{A}_i| \geq \delta} A_i \text{sign}_\delta(\hat{A}_i). \quad (29)$$

Similar to the proof of Theorem 1, we can derive that

$$\dot{V} = - \sum_{i: |\hat{A}_i| \geq \delta} A_i \text{sign}_\delta(\hat{A}_i) \leq - \sum_{i: |\hat{A}_i| \geq \delta} \frac{|\hat{A}_i|}{2} \leq - \sum_{i: |\hat{A}_i| \geq \delta} \frac{\delta}{2}. \quad (30)$$

Then, we can conclude that, with the proposed distributed self-triggered power sharing controller, the control objective (3) can be achieved with the convergence error of $|\sum_{j \in \mathcal{N}_i} a_{ij}(p_i - p_j)| < \delta$. ■

By Theorems 1 and 2, we can achieve both $\omega - P$ secondary control objectives simultaneously only with reduced communication and computation requirements, which will greatly increase the system efficiency of the islanded MGs. Figure 2 illustrates the block diagram of the proposed self-triggered secondary controllers.

4. Verification results

In this section, we validate the effectiveness of the proposed self-triggered secondary controllers by simulating a test MG in MATLAB/Simulation environment. The test MG model consists of four DGs with a circle undirected communication network as depicted in Fig. 3. It should be pointed out that the DG in the test MG is modeled as an

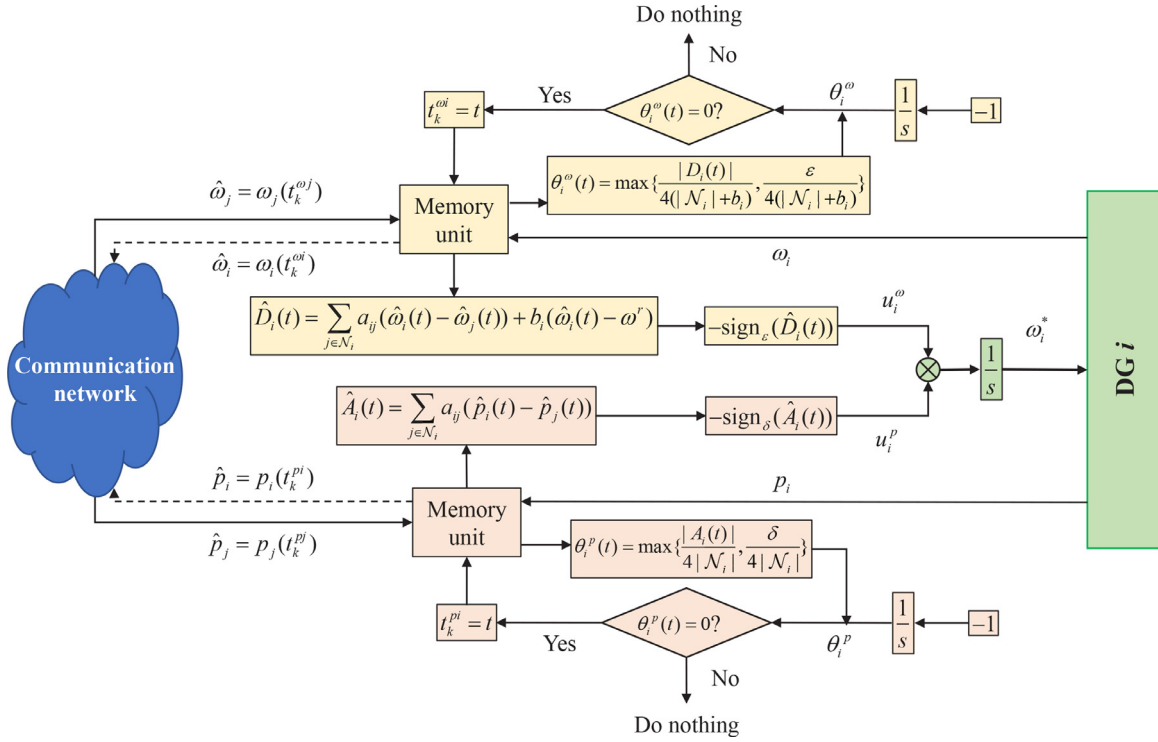


Fig. 2. Block diagram of the proposed self-triggered secondary controllers.

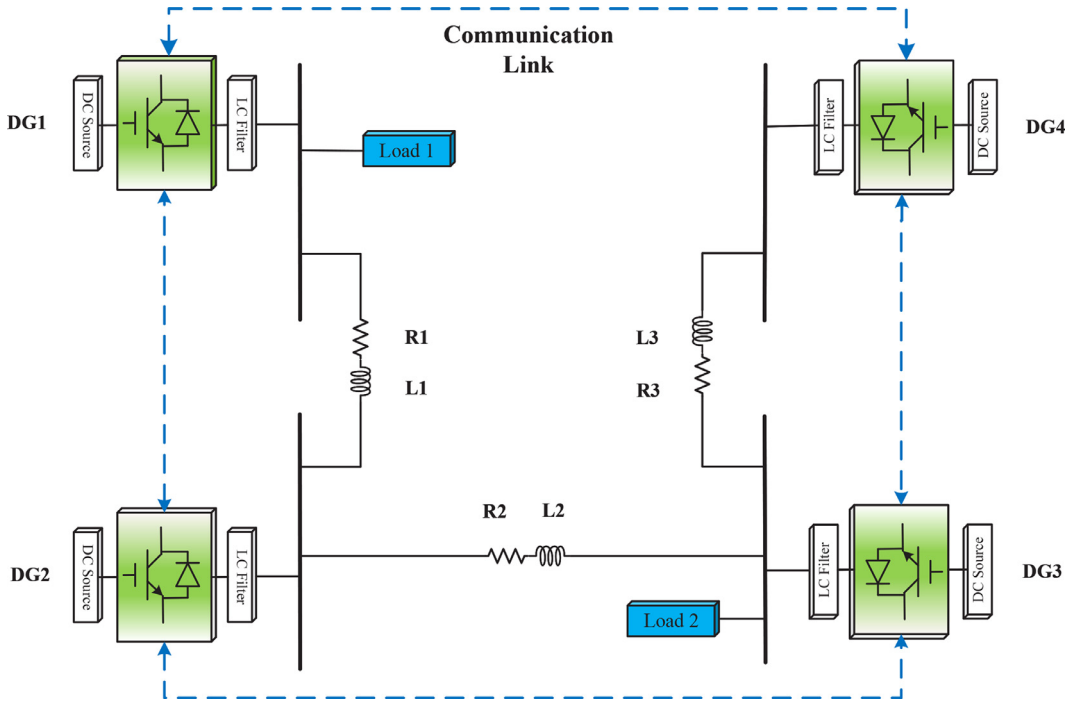


Fig. 3. Single-line diagram of the test MG model.

inverter-based voltage resource that includes the inner voltage and inner power control loops, as well as PWM mechanism simulations. The parameter settings of the test MG are provided in Table 1.

For the frequency restoration and power sharing controllers, the convergence errors are set to be $\varepsilon = \delta = 0.01$. As illustrated later, this setting can meet the convergence requirements of MGs. The reference frequency is set to be $f^r = 50$ Hz, i.e., $\omega^r = 2\pi f^r = 314$ rad/s. The sampling step of the system is discretized to 0.001 s.

We will first show the effectiveness of proposed self-triggered controllers, then the comparisons to the traditional distributed secondary controller (i.e., time-triggered) and to the state-of-the-art event-triggered controller will be provided.

The simulation process is set to be: At $t = 0$ s, the MG isolates from the main grid and works at islanded mode. At the beginning, the MG is only monitored by primary droop control. Then, at $t = 1$ s, the secondary control is started. After that, at $t = 3$ s, Load2 suddenly increases 10 kW.

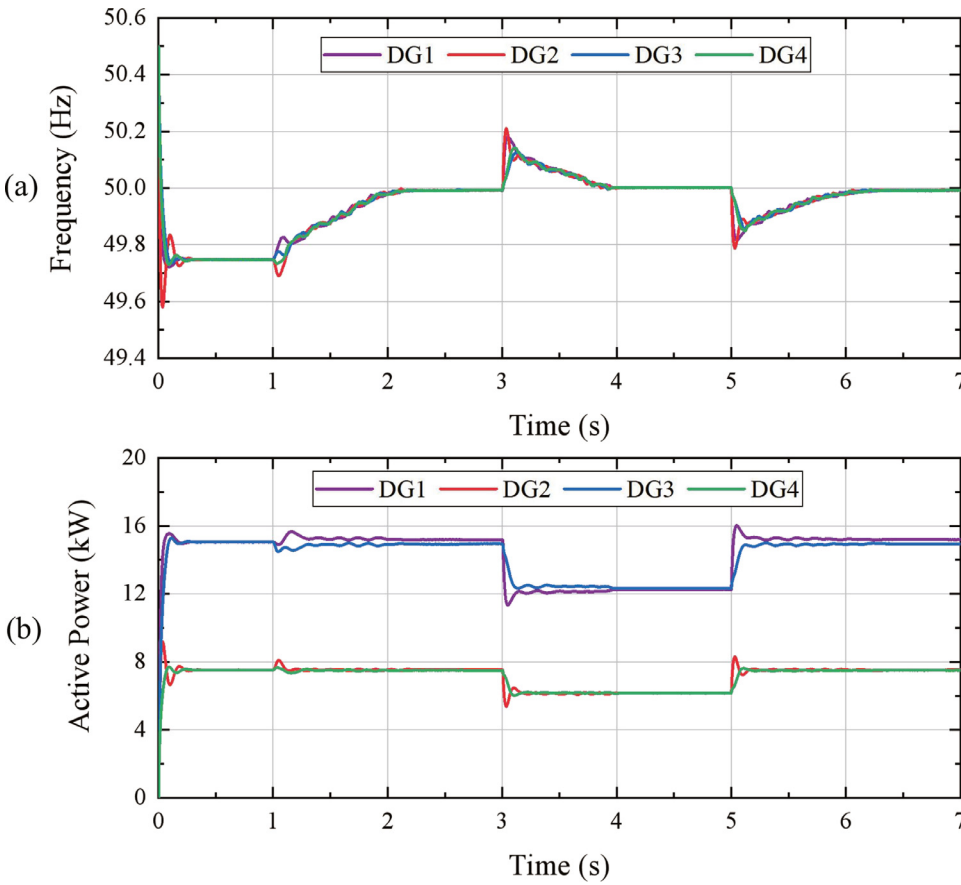


Fig. 4. Performances of the proposed controllers: (a) Frequencies of DGs; (b) Active powers of DGs.

Table 1
Parameter Settings of the Test MG System.

DGs	DG1 & DG3		DG2 & DG4	
	P_{max}	20 kW	P_{max}	10 kW
m_p	5×10^{-5}	m_p	10×10^{-5}	
R_c	0.2 Ω	R_c	0.2 Ω	
L_c	3×10^{-3} H	L_c	3×10^{-3} H	

Lines	Line 1 & Line 3		Line 2	
	$R_1 \& R_3$	0.23 Ω	R_2	0.35 Ω
$L_1 \& L_3$	3.18×10^{-3} H	L_2	1.847×10^{-3} H	

Loads	P_{load1}		P_{load2}	
		30 kW		20 kW

Then, at $t = 5$ s, Load2 drops 10 kW. The total simulation time is set to be 7 s.

4.1. Effectiveness verification

Figure 4 shows the system performance of the proposed self-triggered controllers, where Fig. 4(a) provides the frequencies of DGs and Fig. 4(b) illustrates the output active powers of DGs. It can be observed that, after the MG being islanded, the frequency of the system is quickly stabilized due to the droop-based primary control. The active power is allocated according to each DG's droop coefficient, but the frequency is deviated from the nominal value 50 Hz. While after the secondary controllers are actuated, the frequency of the system is gradually compensated to 50 Hz. And the active power outputs are allocated to remain the same sharing pattern as the droop-based primary control. While after load changes occurring at 3 s and 5 s, the frequency can also be restored back to the nominal value and the active power are shared properly either. It should be noted from Fig. 4(b) that there exists

a small convergence error during the steady states due to the error setting. However, the error is very small, and the system is stable, such that the performance is acceptable for the operation of islanded MGs. This result validates that the proposed self-triggered secondary controllers can achieve the secondary control objectives effectively.

Figure 5 illustrates the triggering time instants of the proposed controllers, in which the numbers on the right-hand side of the sub-figures are the total number of the triggers. It can be seen that the triggers for each DG are aperiodic and intermittent rather than continuously. And the total number of triggers for each DG is only around 200. It can also be found that the triggers during transient processes are very sparse, whereas there exist some triggers during steady states. The triggers during the steady states may be caused by the model error of the test MG, because our MG model contains elaborately modeled DG by involving inner voltage, inner power control loops and PWM control, which would inevitably bring some generation errors. In fact, in the real application environment, despite of the generation error, the measurement noises could also lead to some other errors. These errors would make the outputs of some DGs beyond the allowable convergence error range during steady states, and hence, more triggers are generated. Thus, the simulation result is more in line with practice applications. Nevertheless, the triggering time instants for each DG are highly reduced, which implies the proposed self-triggered secondary controllers can reduce the communication and computation requirement significantly.

Moreover, it can be observed from Figs. 4 and 5 that the curves of the frequencies and the active powers are serrated rather than smooth during the transient process. And the convergence trend of frequency is linear due to the signum function and the linear clock.

4.2. Comparison verification

In this subsection, we compare the proposed distributed self-triggered controller with the traditional distributed controller and a

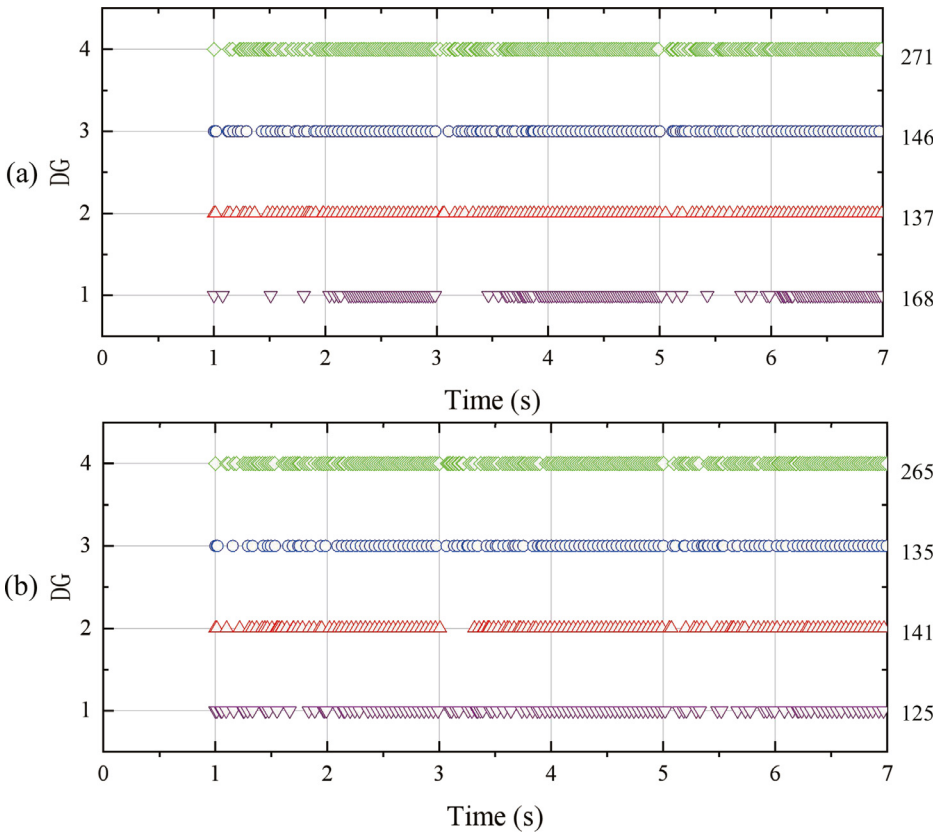


Fig. 5. Triggering time instants: (a) Frequency controller; (b) Active power controller.

state-of-the-art distributed event-triggered controller in [29]. Without loss of generality, we only consider frequency restoration control here to simplify the results.

For the distributed event-triggered controller in [29], the triggering time sequence for the frequency restoration is as follows:

$$t_{k+1}^i = \min_{t > t_k^i} \{t \mid e_i^2(t) \geq \frac{\sigma_i}{4m_i^2} \hat{D}_i^2(t)\}, \quad (31)$$

where $m_i = |\mathcal{N}_i| + \frac{1}{2}d_i$.

There main difference between the proposed self-triggered controller and the event-triggered controller in [29] lines in: 1) the proposed self-triggered controller only needs to monitor the clock θ to see if it decreases to 0. The calculation only occurs at the triggering time to update the linear clock. However, the event-triggered controller in [29] needs to continuously calculating the triggering condition $e_i^2(t) \geq \frac{\sigma_i}{4m_i^2} \hat{q}_i^2(t)$ to see if the trigger should be conducted at current, which results in a huge computation overhead. 2) Without signum function being involved, the event-triggered controller in [29] achieves an exponential convergence.

Figure 6 shows the performances of the traditional time-triggered control, the event-triggered control and the proposed self-triggered con-

trol. It can be seen that our proposed self-triggered controller shows different convergence results in comparison with the traditional controller and the event-triggered controller. The biggest difference between the three controllers appears in the transient process. As shown in Fig. 6(a), the convergence of the traditional controller is smooth. However, for the event-triggered controller and the self-triggered controller, there appear some sawtooth ripples during the convergence periods caused by the event/self-triggered mechanisms as illustrated in the amplification figures in Fig. 6(b) and (c).

Figure 7 provides the triggering time instants of the traditional control, the event-triggered control, and the self-triggered control. As shown in Fig. 7(a), with the traditional control, each DG needs to trigger continuously and conduct 6000 times control actions and 12,000 times communications (each DG has two neighbors). However, as shown in Fig. 7(b) and (c), the triggers of DGs under the event-triggered control and the self-triggered control are more sparse than that of the traditional control, which demonstrates the communication efficiency of the event/self-triggered control. But, the pattern of the triggers in Fig. 7(b) is totally different from Fig. 7(c). It is shown that the self-triggered controller requires fewer communications than the event-triggered con-

Table 2
Comparison results of NC and NTCC.

Controller	Number	DG1	DG2	DG3	DG4
Traditional controller	NC (Times)	12,000	12,000	12,000	12,000
	NTCC (Times)	0	0	0	0
Event-triggered controller	NC (Times)	370	526	582	568
	NTCC (Times)	6000	6000	6000	6000
Self-triggered controller	NC (Times)	336	274	292	547
	NTCC (Times)	0	0	0	0

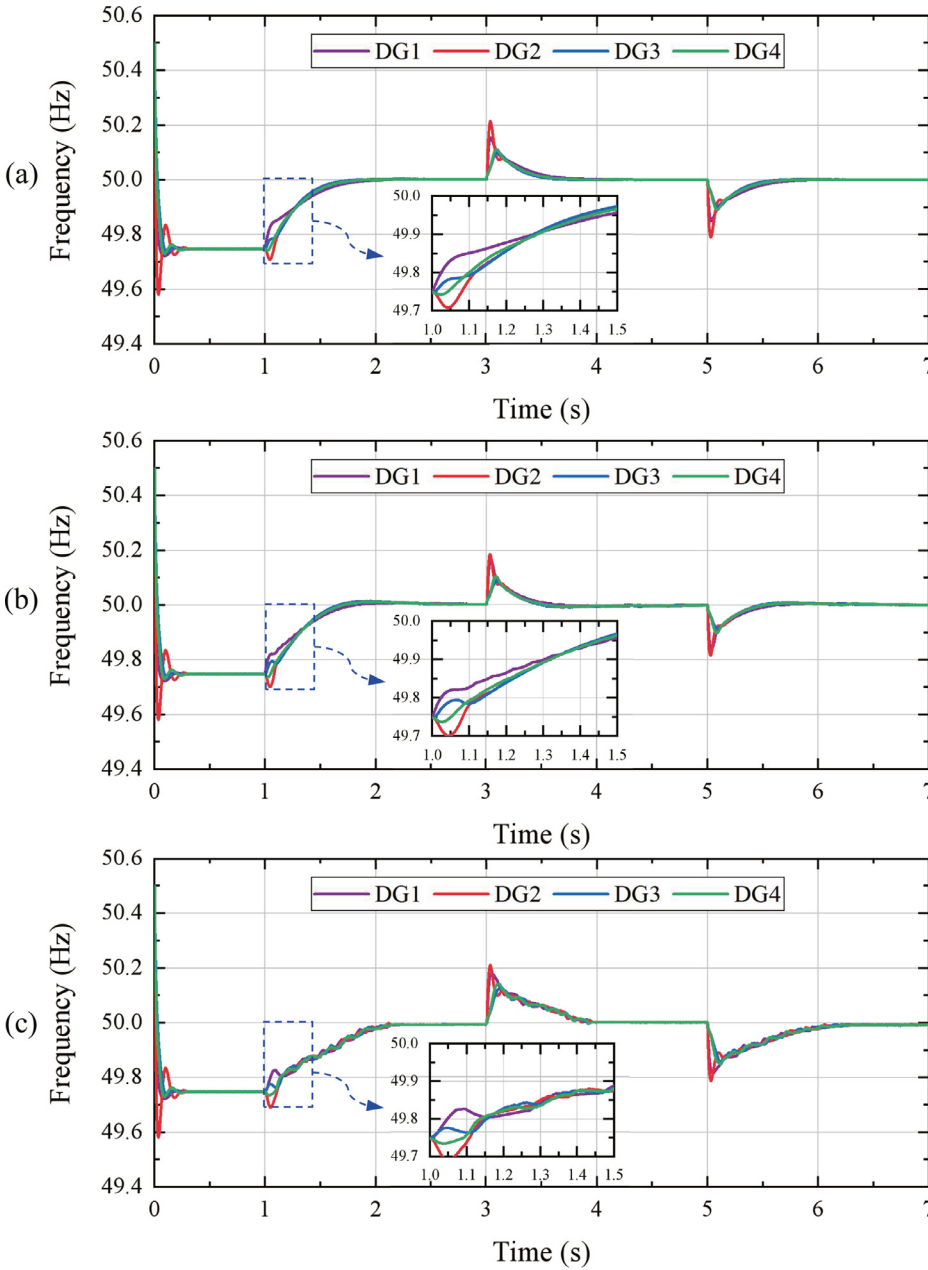


Fig. 6. Frequencies of DGs under the comparison controllers: (a) Traditional controller; (b) Event-triggered controller; (c) Self-triggered controller.

troller during the transient process. However, it triggers more often during steady states due to the measurement error and communication noise. This means that our proposed self-triggered controller is suitable for the system with frequent disturbances, but the event-triggered controller in [29] is more applicable to the system with fewer disturbances. In practice, there always exists small disturbances in power systems. From this perspective, the proposed self-triggered controllers are more applicable in real applications.

Table 2 provides the comparison results associated with the number of communications (NC in the table) and the number of triggering condition computations (NTCC in the table) for the three controllers. It is worth mentioning that, since each DG has two neighbors, the number of communications is twice as much as the number of triggering time instants. From the table, it is also observed that the event-triggered controller and the self-triggered controller significantly reduce the communication cost for each controller compared with the traditional controller, and the self-triggered controller has better per-

formance than that of the event-triggered controller (the reduction is about 96% for the event-triggered controller, about 97% for the self-triggered controller). However, even though the number of communications for the event-triggered controller and the self-triggered controller are in the same quantity, the number of the triggering condition computations of them is different. The event-triggered control requires the controller to compute a complicated triggering condition at each iteration, but the proposed self-triggered control only needs to monitor a simple clock without triggering condition calculation. This indicates that the proposed self-triggered control achieves a lot of computation resource saving, which verifies the superiority of the proposed self-triggered control.

4.3. Performances with different parameter settings

In this subsection, we will show how the selected error ϵ affects the performance of the controller. Since the convergence error is more

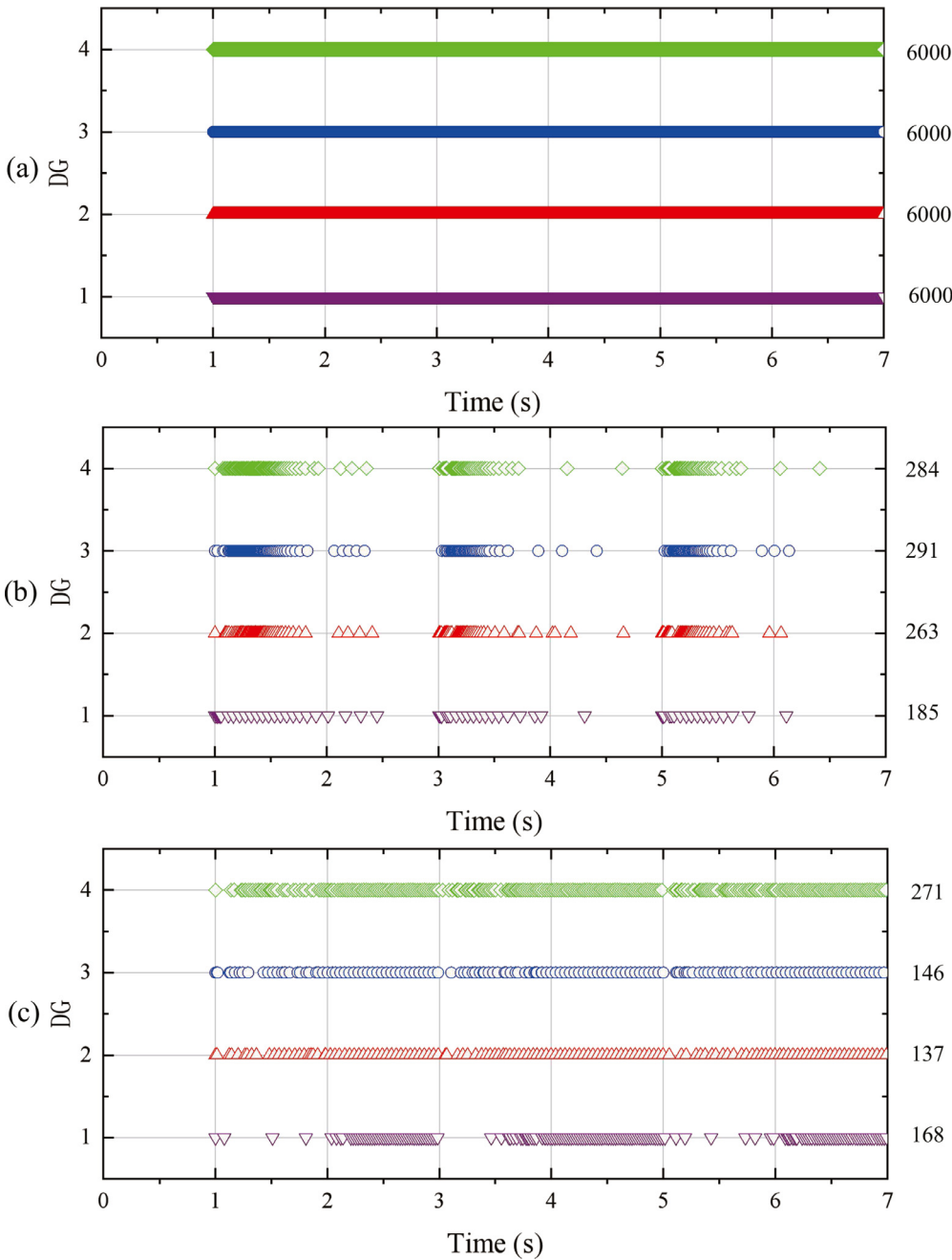


Fig. 7. Triggering time instants: (a) Traditional controller; (b) Event-triggered controller; (c) Self-triggered controller.

apparent in the results of the active power sharing, we only show the active power allocation performances under different error ϵ for conciseness.

Figure 8 illustrates the active power of each DG and the corresponding triggering time instants when the error ϵ is selected to be 0.005, which is smaller than the case in Section 4.1, where ϵ is 0.01. Comparing Fig. 8(a) with Fig. 4(b), it is clearly shown that the active power allocation error becomes smaller due to the smaller ϵ . But, as compared Fig. 8(b) with Fig. 5(b), the smaller ϵ also increases the number of triggering time instants.

Table 3 shows more cases of the controller with different ϵ , in which the largest convergence error and the average number of triggers of the simulation results are provided. From the table, one can observe that the controller with smaller ϵ results in smaller convergence error, but will

Table 3
Performances of the controller with different ϵ .

ϵ	0.05	0.01	0.005	0.001
Convergence error (W)	1330	260	120	20
Average Number of Triggers (Times)	44.25	180.5	286.5	1342.75

generate more triggers. On the contrary, the controller with larger ϵ generates fewer triggers, but will lead to larger convergence error, which coincides with our previous analysis. Therefore, the trade-off between the number of triggering times and the control performance should be considered when designing a distributed self-triggered secondary controller.

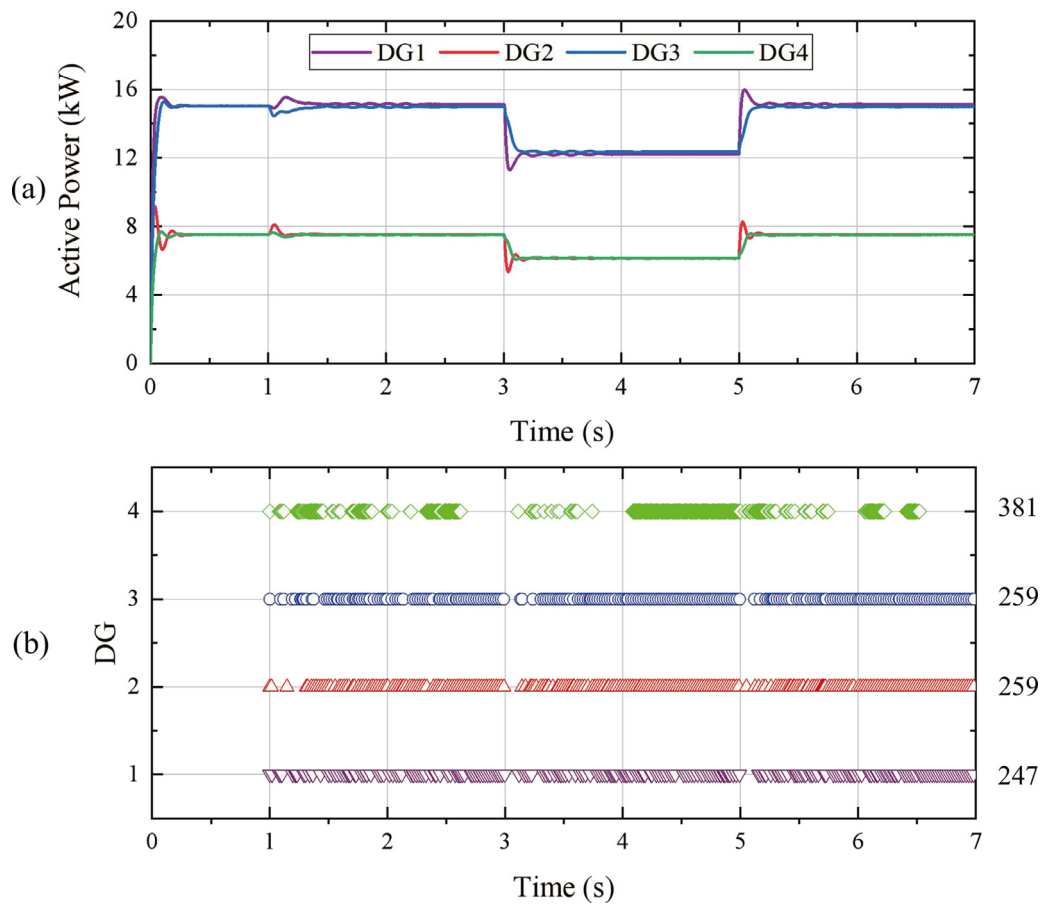


Fig. 8. Control performance: (a) Active power sharing with $\varepsilon = 0.05$; (b) Corresponding triggering time instants.

5. Conclusion

This paper proposes a distributed self-triggered control strategy to coordinate the distributed renewable generators for frequency restoration in microgrids. First, a self-triggered frequency restoration control algorithm is proposed according to the signum function and a designed linear clock. Then, the self-triggered control for active power sharing is realized by a similar design principle as well. It is proved that, with the aid of the linear clock, Zeno behavior can be naturally excluded for each controller. Moreover, each controller does not need to compute any triggering condition. Finally, the verification results show that, compared with traditional distributed secondary control, the proposed self-triggered controller can reduce about 97% communication requirements. And compared with the state-of-the-art distributed event-triggered secondary control, the proposed self-triggered controller not only can achieve similar communication reduction but also can significantly reduce computation costs. Thus, the energy consumption of the control system is reduced as well. Furthermore, it is found that the triggering pattern of the proposed self-triggered controller is different from the state-of-the-art event-triggered controller, our proposed self-triggered controller is more applicable to the system with frequent disturbances, thus is more applicable to real power system. In addition, it is also found that the parameter ε affects the number of triggering times and the control performance. One should select proper ε according to the practical requirements when designing the self-triggered controller. Future work will be focused on how to relax the communication network topology to the general directed graph and how to modify the proposed self-triggered controller into an asymptotical convergence controller for the secondary control in microgrids.

Declaration of Competing Interest

The authors declare that they have no known competing financial interests or personal relationships that could have appeared to influence the work reported in this paper.

Data availability

No data was used for the research described in the article.

Acknowledgement

This paper was supported in part by the [National Natural Science Foundation of China](#) (Grant No. U1909201, 62101490) and the Research Startup Funding from Hainan Institute of [Zhejiang University](#) (Grant No. 0210-6602-A12202).

References

- [1] Yan J. Energy systems in transition: challenges and opportunities. *Adv Appl Energy* 2020;1:100005.
- [2] Zhao N, Zhang H, Yang X, Yan J, You F. Emerging information and communication technologies for smart energy systems and renewable transition. *Adv Appl Energy* 2023;100125.
- [3] Wang C. Analysis and simulation theory of microgrids. Beijing: Science Press; 2013.
- [4] Pong PW, Annaswamy AM, Kroposki B, Zhang Y, Rajagopal R, Zussman G, et al. Cyber-enabled grids: shaping future energy systems. *Adv Appl Energy* 2021;1:100003.
- [5] Yang S, Lao K-W, Hui H, Chen Y, Dai N. Real-time harmonic contribution evaluation considering multiple dynamic customers. *CSEE J Power Energy Syst* 2023. Early Access
- [6] Hui H, Siano P, Ding Y, Yu P, Song Y, Zhang H, et al. A transactive energy framework for inverter-based HVAC loads in a real-time local electricity market considering distributed energy resources. *IEEE Trans Ind Inf* 2022;18(12):8409–21.

- [7] Guerrero JM, Vasquez JC, Matas J, de Vicuna LG, Castilla M. Hierarchical control of droop-controlled AC and DC microgrids—a general approach toward standardization. *IEEE Trans Ind Electron* 2011;58(1):158–72.
- [8] Bidram A, Davoudi A. Hierarchical structure of microgrids control system. *IEEE Trans Smart Grid* 2012;3(4):1963–76.
- [9] Dong Z, Zhang X, Zhang N, Kang C, Strbac G. A distributed robust control strategy for electric vehicles to enhance resilience in urban energy systems. *Adv Appl Energy* 2023;9:100115.
- [10] Khayat Y, Shafiee Q, Heydari R, Naderi M, Dragievi T, Simpson-Porco JW, et al. On the secondary control architectures of AC microgrids: an overview. *IEEE Trans Power Electron* 2020;35(6):6482–500.
- [11] Xin H, Qu Z, Seuss J, Maknouninejad A. A self-organizing strategy for power flow control of photovoltaic generators in a distribution network. *IEEE Trans Power Syst* 2010;26(3):1462–73.
- [12] Bidram A, Davoudi A, Lewis FL, Qu Z. Secondary control of microgrids based on distributed cooperative control of multi-agent systems. *IET Gen Transm Distrib* 2013;7(8):822–31.
- [13] Bidram A, Lewis FL, Davoudi A. Distributed control systems for small-scale power networks: using multiagent cooperative control theory. *IEEE Control Syst Mag* 2014;34(6):56–77.
- [14] Zhang G, Li C, Qi D, Xin H. Distributed estimation and secondary control of autonomous microgrid. *IEEE Trans Power Syst* 2016;32(2):989–98.
- [15] Hui H, Chen Y, Yang S, Zhang H, Jiang T. Coordination control of distributed generators and load resources for frequency restoration in isolated urban microgrids. *Appl Energy* 2022;327:120116.
- [16] Ajagekar A, Mattson NS, You F. Energy-efficient ai-based control of semi-closed greenhouses leveraging robust optimization in deep reinforcement learning. *Adv Appl Energy* 2023;9:100119.
- [17] Fan Y, Hu G, Egerstedt M. Distributed reactive power sharing control for microgrids with event-triggered communication. *IEEE Trans Control Syst Technol* 2017;25(1):118–28.
- [18] Chen M, Xiao X, Guerrero JM. Secondary restoration control of islanded microgrids with a decentralized event-triggered strategy. *IEEE Trans Ind Inf* 2018;14(9):3870–80.
- [19] Chen Y, Qi D, Li Z, Wang Z, Yang X, Zhang J. Distributed event-triggered control for frequency restoration in islanded microgrids with reduced trigger condition checking. *CSEE J Power Energy Syst* 2021. Early Access
- [20] Weng S, Yue D, Dou C, Shi J, Huang C. Distributed event-triggered cooperative control for frequency and voltage stability and power sharing in isolated inverter-based microgrid. *IEEE Trans Syst Man Cybern* 2019;49(4):1427–39.
- [21] Abdolmaleki B, Shafiee Q, Arefi MM, Dragičević T. An instantaneous event-triggered Hz–Watt control for microgrids. *IEEE Trans Power Syst* 2019;34(5):3616–25.
- [22] Dimarogonas DV, Frazzoli E, Johansson KH. Distributed event-triggered control for multi-agent systems. *IEEE Trans Automat Contr* 2012;57(5):1291–7.
- [23] Wang Y, Nguyen TL, Xu Y, Li Z, Tran Q, Caire R. Cyber-physical design and implementation of distributed event-triggered secondary control in islanded microgrids. *IEEE Trans Ind Appl* 2019;55(6):5631–42.
- [24] Abdolmaleki B, Shafiee Q, Seifi AR, Arefi MM, Blaabjerg F. A zero-free event-triggered secondary control for ac microgrids. *IEEE Trans Smart Grid* 2020;11(3):1905–16.
- [25] Xie Y, Lin Z. Distributed event-triggered secondary voltage control for microgrids with time delay. *IEEE Trans Syst Man Cybern Syst* 2019;49(8):1582–91.
- [26] Choi J, Habibi SI, Bidram A. Distributed finite-time event-triggered frequency and voltage control of AC microgrids. *IEEE Trans Power Syst* 2022;37(3):1979–1994.
- [27] Qian Y-Y, Premakumar AVP, Wan Y, Lin Z, Shamash YA, Davoudi A. Dynamic event-triggered distributed secondary control of DC microgrids. *IEEE Trans Power Electron* 2022;37(9):10226–38.
- [28] Wang S, Hui H, Ding Y, Ye C, Zheng M. Operational reliability evaluation of urban multi-energy systems with equivalent energy storage. *IEEE Trans Ind Appl* 2022:1–15.
- [29] Chen Y, Li C, Qi D, Li Z, Wang Z, Zhang J. Distributed event-triggered secondary control for islanded microgrids with proper trigger condition checking period. *IEEE Trans Smart Grid* 2022;13(2):837–48.
- [30] Chen Y, Lao K-W, Qi D, Hui H, Yang S, Yan Y, et al. Distributed self-triggered control for frequency restoration and active power sharing in islanded microgrids. *IEEE Trans Ind Inf* 2022;1(1). 1–1
- [31] De Persis C, Frasca P. Robust self-triggered coordination with ternary controllers. *IEEE Trans Automat Contr* 2013;58(12):3024–38.
- [32] Wu H, Pratt A, Munankarmi P, Lunacek M, Balamurugan SP, Liu X, et al. Impact of model predictive control-enabled home energy management on large-scale distribution systems with photovoltaics. *Adv Appl Energy* 2022;6:100094.
- [33] Chen Y, Qi D, Dong H, Li C, Li Z, Zhang J. A FDI attack-resilient distributed secondary control strategy for islanded microgrids. *IEEE Trans Smart Grid* 2021;12(3):1929–38.
- [34] Wang Y, Deng C, Liu D, Xu Y, Dai J. Unified real power sharing of generator and storage in islanded microgrid via distributed dynamic event-triggered control. *IEEE Trans Power Syst* 2021;36(3):1713–24.
- [35] Bidram A, Davoudi A, Lewis FL, Guerrero JM. Distributed cooperative secondary control of microgrids using feedback linearization. *IEEE Trans Power Syst* 2013;28(3):3462–70.
- [36] Wang Y, Nguyen TL, Xu Y, Shi D. Distributed control of heterogeneous energy storage systems in islanded microgrids: finite-time approach and cyber-physical implementation. *Int J Electr Power Energy Syst* 2020;119:105898.
- [37] Nowzari C, Cortes J. Distributed event-triggered coordination for average consensus on weight-balanced digraphs. *Automatica* 2016;68(68):237–44.